Cell behaviour on micropatterned substrata: limits of extracellular matrix geometry for spreading and adhesion

Dirk Lehnert[1], Bernhard Wehrle-Haller[2], Christian David[3], Ulrich Weiland[1], Christoph Ballestrem[2], Beat A. Imhof[2] and Martin Bastmeyer[1,*]

[1] Department of Biology, University of Konstanz, Universitaetstrasse 10, 78457 Konstanz, Germany
[2]Department of Pathology, Centre Medical Universitaire, Geneva, Switzerland
[3]Laboratory for Micro- and Nanotechnology, Paul Scherrer Institut, Villigen-PSI, Switzerland
*Author for correspondence at present address: Friedrich-Schiller-Universität, Institut für Allgemeine Zoologie, Erbertstrasse 1, 07743 Jena, Germany (e-mail: bastmeyer@pan.zoo.uni-jena.de)

Accepted 18 August 2003
Journal of Cell Science 117, 41-52 Published by The Company of Biologists 2004
doi:10.1242/jcs.00836

Summary

Cell adhesion, spreading and migration require the dynamic formation and dispersal of contacts with the extracellular matrix (ECM). In vivo, the number, availability and distribution of ECM binding sites dictate the shape of a cell and determine its mobility. To analyse the geometrical limits of ECM binding sites required for cell attachment and spreading, we used microcontact printing to produce regular patterns of ECM protein dots of defined size separated by nonadhesive regions. Cells cultured on these substrata adhere to and spread on ECM regions as small as 0.1 μm^2, when spacing between dots is less than 5 μm. Spacing of 5-25 μm induces a cell to adapt its shape to the ECM pattern. The ability to spread and migrate on dots ≥1 μm^2 ceases when the dot separation is ≥30 μm. The extent of cell spreading is directly correlated to the total substratum coverage with ECM-proteins, but irrespective of the geometrical pattern. An optimal spreading extent is reached at a surface coating above 15%. Knowledge of these geometrical limits is essential for an understanding of cell adhesion and migration, and for the design of artificial surfaces that optimally interact with cells in a living tissue.

Key words: Microcontact printing, Patterned substratum, Focal adhesion, Integrin, Cytoskeleton

Introduction

Cell adhesion involves the interaction of cells with other cells or with the extracellular matrix (ECM) and is of great importance in the development and disease of multicellular organisms (Gumbiner, 1996). The initial phase of cell-matrix interaction is characterized by the binding of integrin receptors (Hynes, 1992) to ECM molecules and the lateral aggregation of receptors at these contact sites (Miyamoto et al., 1995). This leads to the induction of intracellular signalling cascades that cause the recruitment of specific molecules linking the actin cytoskeleton via integrins to the ECM (Burridge and Chrzanowska-Wodnicka, 1996; Yamada and Miyamoto, 1995). These cell/matrix adhesions are also the sites at which contractile forces produced inside the cell are exerted onto the substratum (Sheetz et al., 1998; Balaban et al., 2001) and, consequently, their distribution dictates the size and shape of the cell (Ingber, 1997). Fibroblast-like cells develop adhesion sites that vary in size and shape. They are referred to as focal complexes, focal contacts or fibrillar adhesions (reviewed by Geiger et al., 2001). Since the characteristics of the different adhesion sites vary with respect to culture conditions and between cell types, we will generally use the term ‘focal adhesions’ throughout this paper.

The types of ECM architecture that cells encounter in vivo range from the homogeneous meshwork of basement membranes to the fibrillar scaffold of connective tissue or healing wounds. A cell is therefore confronted either with nanopatterned surfaces (Abrams et al., 2000) or with fibrils of ECM proteins spaced in the μm range (Wezemann, 1998). Most of our current knowledge of cell matrix adhesions is based on in vitro studies of cells growing on homogeneously coated culture dishes (reviewed by Zamir and Geiger, 2001; Geiger et al., 2001; Geiger and Bershadsky, 2002; Wehrle-Haller and Imhof, 2002). Although this strategy has led to important findings, it is not an exact representation of the in vivo situation. More recently, fibroblast adhesion has been studied in three-dimensional ECM matrices derived from tissues or cell cultures. However, exact analysis of cell behaviour is hampered by the poorly defined geometry of the used ECM matrices (Cukierman et al., 2001). To understand in more detail how cell behaviour is dictated by the architecture of the ECM, we exposed cells to geometrically patterned two-dimensional substrata of ECM molecules obtained by the micro-contact-printing technique [μCP (reviewed by Mrksich and Whitesides, 1996)]. Using this method, patterns of self-assembled monolayers of alkanethiols on gold surfaces that either support or prevent protein binding can be produced (Prime and Whitesides, 1991). The desired patterns were created using computer software and transferred to a silicon wafer (master) by lithographic techniques. An elastic

polydimethylsiloxane (PDMS) stamp is then produced from the master, inked with the adhesive alkanethiol and pressed onto a gold-coated coverslip (Fig. 1A). After filling the uncoated regions with the non-adhesive alkanethiol, the coverslip is coated with ECM molecules, thus producing a well-defined patterned substratum (Fig. 1A).

Using μCP, Ingber and co-workers (Chen at al., 1997) produced round islands of ECM proteins as small as 3 μm in diameter. They found that the long-term effect of cell shape on growth and survival is not a consequence of the total cell/ECM contact area, but is regulated through changes in cell tension and architecture (Chen et al., 1997). In the present study, we have analysed the influence of ECM patterns in the micrometer range during the initial phases of cell adhesion and spreading by controlling the size of ECM squares (0.3-3 μm square) and the distance between them (1-30 μm, centre to centre). Although additional factors like other ECM proteins or the concentration of ECM coating might also influence cell behaviour, we found a clear relationship between cell behaviour and substratum geometry. We show that cells integrate the pattern of ECM to which they are exposed by regulating the amount of focal adhesions formed, in order to maintain their spread shape. This adaptation occurs within a certain range of surface coverage and ECM spacing. For the investigated cell lines, the limits are a maximal distance of 25 μm between adhesive surfaces and an ECM coating of 5-8% for half maximal spreading. ECM dots as small as 0.1 μm^2 can still induce the formation of focal adhesions bur do not support spreading when spaced at more than 5 μm.

Knowing these geometrical limits will allow a better understanding of in vivo cell behaviour in situations such as embryogenesis, wound healing and fibroblast migration. It will be essential for the design of implants with artificial surfaces allowing optimal interaction with cells in a tissue.

Materials and Methods

Microcontact printing

Masters for microcontact printing were fabricated from silicon wafers by low voltage electron beam lithography using a positive tone resist (David and Hambach, 1999). The resulting resist pattern was inverted using a lift-off process and reactive ion etching (David and Souvorov, 1999) to yield a master with rectangular, 650 nm deep holes in the silicon surface. We designed the master pattern in such a way that several 500×000 μm areas with the different dot patterns were separated by 50 μm unexposed areas to mechanically support the silicon stamp during printing (Fig. 1B). Silicone stamps were produced by the thin stamp technique (James et al., 1998; Geissler et al., 2000) using Sylgard 184 (Dow Corning). The procedure for microcontact printing is summarised in Fig. 1A. The stamp was 'inked' with a 1.5 mM solution of a hydrophobic alkanethiol [octadecylmercaptan (ODM) Aldrich] in ethanol and pressed onto a gold-coated coverslip, forming self-assembled monolayers at the protruding parts of the stamp (Mrksich et al., 1997). Uncoated regions of the coverslip were blocked with a solution of a hydrophilic alkanethiol [tri-(ethyleneglycol)-terminated alkanethiol; kindly provided by Dr Eck, University of Heidelberg] in ethanol. Protein solutions of ECM molecules in phosphate-buffered saline (PBS; 10 μg/ml fibronectin, Gibco; 5 μg/ml vitronectin, Sigma) were applied to the coverslips for 1 hour at 4°C and bound specifically to the ODM via hydrophobic interaction. Coverslips were then blocked in 1% bovine serum albumin (BSA; Sigma) in Dulbecco's modified Eagle's medium (DMEM; Gibco).

Scanning force microscopy (SFM)

Patterned substrata were prepared and coated with fibronectin as described above, glued to a steel support and transferred to the SFM without drying. The surface was imaged in PBS with a Digital Instruments Multimode MMAFM-2 equipped with a Nanoscope IIIa Controller unit, a JV-Scanner (120 μm lateral scan range) and a Digital Instruments liquid cell (without using the O-ring). Olympus sensor chips (OMCL-RC-800PS-2) with rectangular cantilevers, a nominal force constant of 0.05 N/m and 0.09 N/m and sharpened silicon nitride tips were used. The surface was imaged in contact mode under minimal loading force. SFM images were analysed using the image processing utilities of the Nanoscope software.

Cell culture

Mouse B16F1 melanoma cells (B16 cells) were kindly provided by G. Nicholson (Houston, TX, USA), β3-integrin-EGFP transfected B16 cells (β 3-GFP cells) were produced as described elsewhere (Ballestrem et al., 2001), buffalo rat liver cells (BRL cells) and NIH 3T3 fibroblasts were from American Type Tissue Culture Collection (ATCC). All cell types were grown in Dulbecco's Modified Eagle Medium (DMEM; Gibco) supplemented with 10% FCS under humidified atmosphere and 10% CO_2. Cells were washed two times with PBS (Ca^{2+}- and Mg^{2+}-free) and removed from tissue culture plates (B16 cells mechanically by knocking off the plates and BRL cells and NIH 3T3 fibroblasts by treatment with Hank's Balanced Salt Solution (HBSS; containing 0.1% trypsin and 4 mM EDTA) for 3 minutes. Dissociated cells were washed in DMEM without FCS for 3 minutes, centrifuged and seeded on the patterned substrata in DMEM without FCS (1×10^4 cells/cm^2) and cultured for 1 hour (or 10 minutes).

Immunostaining

Cells were fixed for 10 minutes with 4% paraformaldehyde, 0.01% glutaraldehyde in phosphate buffer, washed three times for 5 minutes with PBS containing 0.1% Triton X-100 (PBST) and incubated with primary antibodies for 1 hour at room temperature or overnight at 4°C. The following primary antibodies were used: polyclonal anti-fibronectin, monoclonal (mAb) anti-vitronectin, mAb anti-talin, mAb anti-vinculin (all from Sigma), mAb anti-FAK, mAb anti-paxillin (BD Transduction Lab), mAb anti-phosphotyrosine (Santa Cruz Biotechnology). Actin filaments were labelled with either Alexa488- or Alexa546-coupled phalloidin (Molecular Probes). Probes were washed three times for 5 minutes with PBST and incubated for 1 hour at room temperature with secondary antibodies. The appropriate fluorescently coupled secondary antibodies (AMCA, Alexa488, Cy3, Cy5) were obtained from Dianova or Molecular Probes. Slides were mounted in Mowiol containing 1% N-propyl-gallate and analysed with a laser scanning microscope (LSM 510, Zeiss). Images were further processed using Adobe Photoshop software.

Quantification of cell spreading

The three different cell types were cultured on patterned fibronectin substrata for 1 hour and labelled for actin and fibronectin. Since protruding parts of the silicone stamps may be slightly deformed during the microcontact printing process, actual sizes of ECM dots can differ from expected sizes as deduced from the master structure. Therefore, actual dot sizes and actual distances between dots were measured from the fibronectin staining using Zeiss LSM software for each quantitative experiment. The fibronectin coverage of the surface was then calculated for each pattern. Uncoated substrata were set as 0% and homogeneously coated substrata as 100% fibronectin coverage. The area covered by single cells on different patterns (10 cells/pattern) was measured from fixed and actin-labelled cells. The outline of the cells, as defined by the actin staining, was drawn around using the Zeiss LSM software and the area calculated.

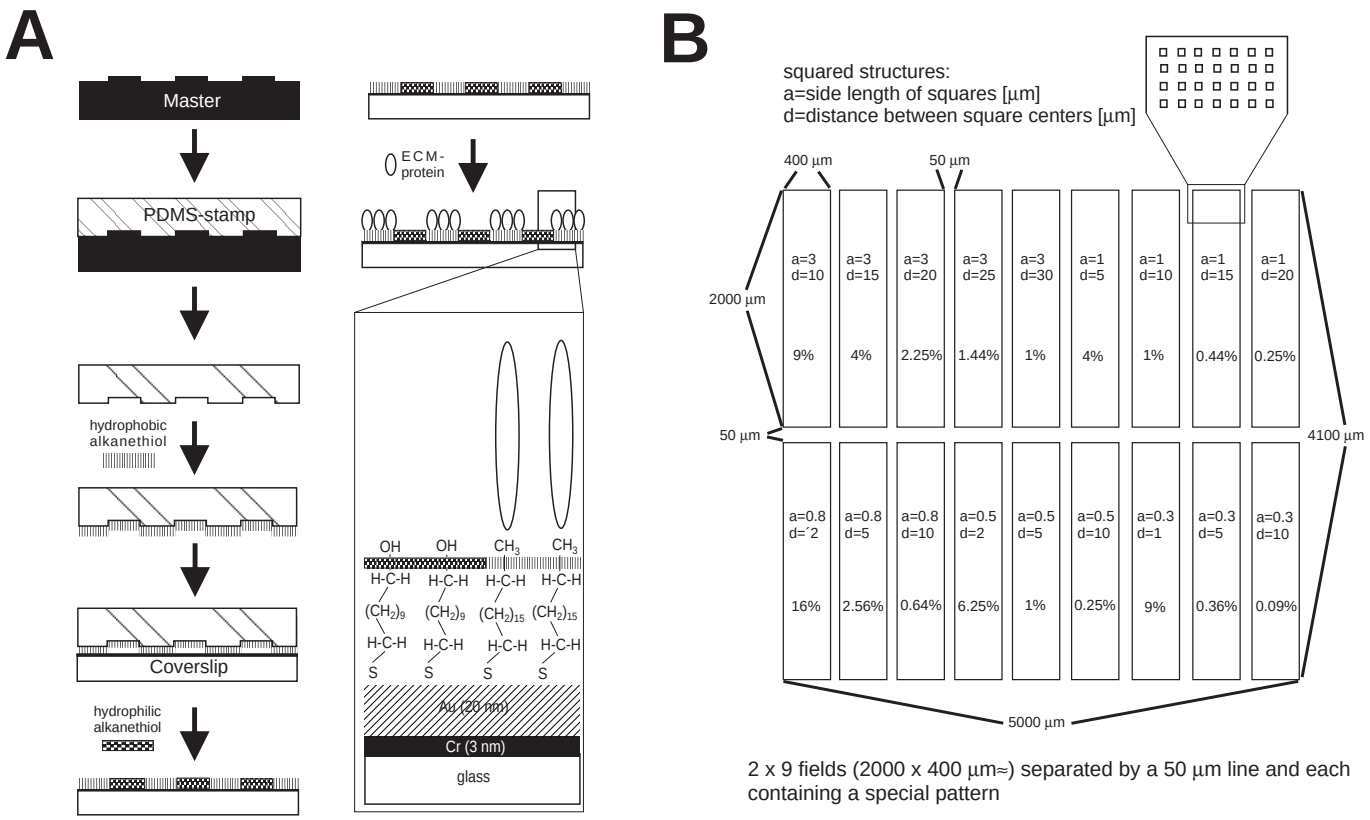

Fig. 1. Schematic of the microcontact printing method. (A) A PDMS stamp is prepared from a silicon master structure and 'inked' with a hydrophobic alkanethiol. The thiol pattern is stamped onto a gold-coated coverslip, forming self-assembled monolayers. The remaining regions are blocked with a protein-resistant hydrophilic alkanethiol. ECM proteins now selectively adsorb to the hydrophobic areas of the coverslip. (B) The PDMS stamp used in this study consists of 2×9 fields, each containing a unique arrangement of squared dots varying in size and distance (a, length of dots in µm; d, centre to centre distance of dots in µm). The theoretical protein coverage for each field is given as a percentage.

Quantification of dot usage

B16 wild-type cells were cultured on patterned fibronectin substrata for 1 hour and labelled for fibronectin, actin and either phosphotyrosine or paxillin as described above. The actual dot sizes (1 μm^2, 3 μm^2, 12 μm^2) and absolute adhesion area according to phosphotyrosine and paxillin staining, respectively, were measured using Zeiss LSM software. A region of interest (ROI) was created using a contour selection tool. Within this ROI both red and green fluorescence were quantified. Laser intensity was set so that the unprocessed images were within the dynamic range, with no pixels saturated. On each pattern the sizes of 12 adhesion sites in peripheral regions of the lamellipodia of four different cells were determined. The relation (adhesion size/dot size × 100) was termed 'dot usage' (%). On substrata coated homogeneously with fibronectin, the size of phosphotyrosine- or paxillin-positive areas in peripheral lamellipodia of the cells was measured in the same way and dot usage calculated.

Time lapse videomicroscopy

Time-lapse studies were performed as described elsewhere (Ballestrem et al., 1998). Briefly, B16 β3-GFP cells were seeded onto patterned fibronectin substrata and incubated for 10 minutes in the incubator. To visualise the dot pattern, 10% fluorescently labelled BSA (Alexa546 protein labelling kit, Molecular Probes) was mixed with the untreated fibronectin molecules during the substratum coating procedure. Cells and pattern were visualised on an Axiovert TV inverted microscope (Zeiss), equipped with an incubation chamber, standard filter sets (Omega) and a Hamamatsu C4742-95-10 digital CCD camera. Images were recorded at intervals of 30 seconds and processed using Openlab software (Improvision).

Results

Characterization of substratum properties

In the present study we used microcontact printing to produce geometrical patterns of ECM proteins (fibronectin, vitronectin) separated by nonadhesive, protein-free regions. By controlling the size of square protein dots in the micrometer and submicrometer range (0.3-3 µm square) and a centre-to-centre distance of 1-30 µm, we created substrata with defined distributions of ECM proteins (Fig. 1B). Immunolabelling of these patterns revealed that ECM dots as small as 0.1 μm^2 (0.3×0.3 µm) can reliably be produced. The actual size of the ECM dots varied slightly between individual experiments, probably because of different pressure forces during the transfer process of alkanethiols from the silicone stamp to the coverslips. The actual size of the dot patterns was therefore always measured using the LSM for each quantitative experiment.

To assess the protein adsorption on the patterned substrata in more detail, scanning force microscopy (SFM) was applied. Fig. 2 shows a SFM image of a patterned substratum with an array of 1 μm^2 dots (actual length 1.2 µm, at a distance of 5 µm). The area between the dots was almost free of

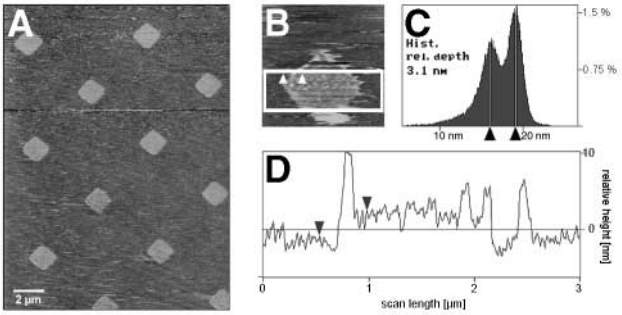

Fig. 2. Protein adsorption on micropatterned substrata. Scanning force microscopy of a micropatterned substratum coated with fibronectin (dots of 1.2 μm square at a distance of 5 μm). (A) Low magnification scan (scan rate 0.5 Hz, total z scale 15 nm) showing that fibronectin is almost exclusively adsorbed to the hydrophobic alkanethiol dots. (B) Higher magnification scan of a fibronectin-coated dot. (C) Bearing histogram of the boxed region in B reveals a mean height difference between the fibronectin-coated area and the surrounding surface of approximately 3 nm. (D) Height profile (line and arrowheads in B; 3×3 μm^2 scan, scan rate 1.5 Hz) showing that fibronectin is adsorbed mainly as a monolayer, but up to three layers can be measured.

adsorbed protein, whereas the covering of the dots with fibronectin appeared to be nearly complete. In accordance with the approximate thickness of the fibronectin molecule [2-3 nm (Engel et al., 1981)], fibronectin is adsorbed mainly as a monolayer (Fig. 2C,D). In some areas a second and a third layer can be observed (Fig. 2D). Fig. 2B also reveals that, despite the minimised loading force, a part of the protein is displaced in scan direction by the tip. A higher loading force applied to remove loosely adsorbed protein resulted in a reduction of the surface covering to about 40-60%. This was roughly estimated from the bearing ratio of those parts of the dot image, with height values higher than the fluctuations of the relatively rough gold-alkanethiol surface (not shown). Smaller dots of 0.25 or 0.1 μm^2 spaced at 5 μm are not easy to detect by AFM and therefore we were unable to perform a statistical analysis of fibronectin coverage. However, the 0.1 μm^2 dots that were successfully scanned showed the same properties as large dots. In addition, we quantified the fibronectin coverage using immunofluorescence and confocal microscopy and found that 0.1 μm^2 dots contain roughly 25% less fibronectin coverage than 1 μm^2 dots.

Thus μCP is a versatile and reliable method for producing patterned substrata with protein-coated dots in the submicrometer range and a homogeneous distribution of ECM-proteins on the dots.

Cells form functional contact sites on μCP patterned ECM substrata

To study the behaviour of cells cultured on patterned ECM substrata, we performed experiments with the following cell lines: stationary 3T3 fibroblasts, migrating B16 F1 melanoma cells and BRL fibroblast-like cells. When these cell types are seeded onto the patterned substrata, they rapidly adhere and start spreading after 10-15 minutes. Fig. 3 shows a B16 melanoma cell after 1 hour on a patterned substratum of 1 μm^2 fibronectin dots. The cell adapts to the geometrical pattern

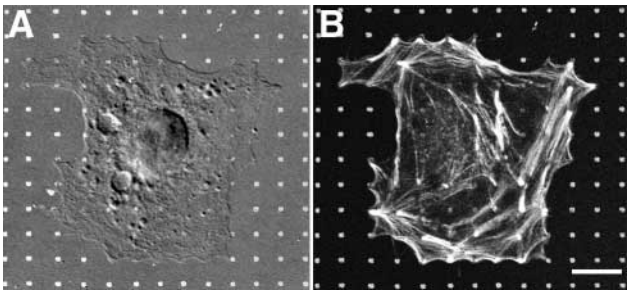

Fig. 3. Cell spreading on micropatterned substrata. A B16 mouse melanoma cell cultured for 1 hour on a patterned substratum of fibronectin. (A) Overlay of fibronectin immunofluorescence (white dots: 1 μm^2; dot distance centre to centre: 5 μm) on a differential interference contrast image. The substratum determines the cell shape, resulting in a rectangular morphology. (B) Overlay of the fibronectin pattern and phalloidin staining reveals that most actin fibres terminate at fibronectin dots. Scale bar: 10 μm.

displaying right angles and straight edges (Fig. 3A). Actin bundles form and span regions between neighbouring dots (Fig. 3B), indicating that functional focal adhesions were created that resisted intracellular acto-myosin tension.

Cell spreading was done in the absence of serum in order to exclude substratum-independent spreading signals (such as growth factors) from our assay. In addition, cells were not allowed to interact with the patterned substrata for more than 1-2 hours, in order to minimise the modification of the substratum pattern by secretion and synthesis of ECM components by the cells. We further analysed the molecular compositions of cell-substratum contacts formed on patterned ECM substrata under these conditions. Focal adhesions normally contain a multitude of cytoskeletal and signal transduction molecules that specifically accumulate at these sites (Zamir and Geiger, 2001). The most representative of these are paxillin, talin and vinculin as markers for cytoskeletal proteins and phosphotyrosine and focal adhesion kinase (FAK) as signal transduction molecules. When cells are cultured on a homogeneous substratum of fibronectin prepared with μCP, they spread normally, similar to their behaviour on ECM-coated glass coverslips (Geiger et al., 2001). On these homogeneous substrata, staining for molecules such as paxillin (not shown) or vinculin (Fig. 4A) are found in a typical pattern at the cell periphery of either small, dot-like adhesions or larger, elongated structures mainly at the cell periphery. Most vinculin-positive foci were connected to actin bundles (Fig. 4A). The intracellular distribution of focal adhesion molecules dramatically changed when cells were cultured on patterned ECM substrata. Vinculin (Fig. 4B) and paxillin (Fig. 4E) were now strictly localised to regions of the cell overlying ECM-coated dots. Marker molecules for signal transduction also accumulate over ECM-dots. Phosphotyrosine staining was associated with almost all dots covered by the cell (Fig. 4D), whereas FAK was mainly concentrated over peripheral dots (Fig. 4C). This accumulation of focal adhesion molecules over the ECM dots occurred rapidly and was already visible 10 minutes after plating (not shown).

Integrins are the key linker proteins that bind the cytoskeleton to the ECM (Hynes, 1992). They assemble into focal adhesions at sites of cell anchoring (Burridge and

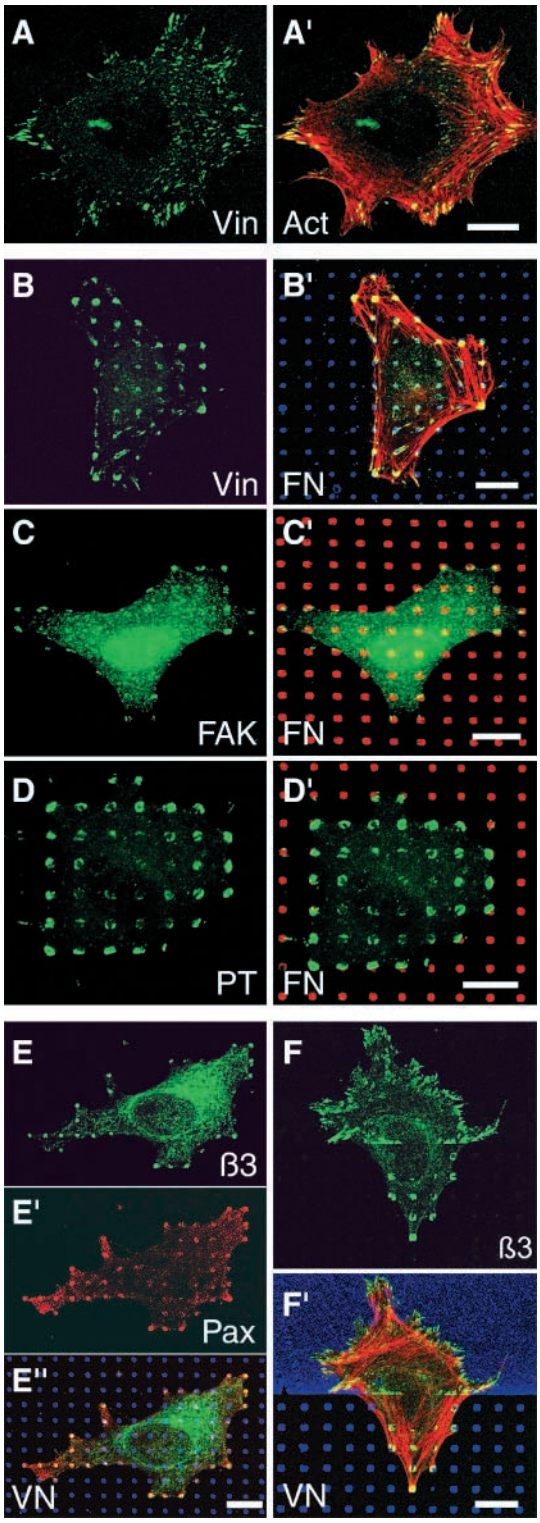

Fig. 4. Molecular composition of focal contacts on micropatterned substrata. B16 cells were cultured for 1 hour on patterned ECM substrata and labelled for focal adhesion molecules and ECM proteins. (A,A′) Cell on a homogenous fibronectin substratum prepared with μCP. Fluorescence staining for vinculin (Vin, green) and actin (Act, red) reveals a staining pattern of dot-like or elongated adhesion foci mainly at the cell periphery that were connected to actin bundles. (B,B′) Cell stained for vinculin (Vin, green) and actin (red) on a patterned substratum of 0.6 μm^2 fibronectin dots (FN, blue). Vinculin has accumulated in areas of the cell overlying ECM dots. Actin fibres terminate in most of these adhesion sites, indicating functional contact sites. (C,C′) Cell stained for focal adhesion kinase (FAK, green) on a patterned substratum of 1 μm^2 FN dots (red). (D,D′) Cell stained for phosphotyrosine (PT, green) on a patterned substratum of 1 μm^2 FN dots (red). (E,E′,E″) B16 cell expressing β3-integrin-GFP (green) stained for paxillin (Pax, red) on a patterned vitronectin (VN, blue) substratum of 0.6 μm^2 dots. (F,F′) B16 cell expressing β 3-integrin-GFP (green) labelled for actin (red) growing on vitronectin (blue) at the border between a uniform and a patterned substratum of 1 μm^2 dots. Note the redistribution of integrin receptors on the patterned substratum. Scale bars: 10 μm.

Chrzanowska-Wodnicka, 1996). The distribution of $\alpha_v\beta_3$ integrin, a receptor for fibronectin and vitronectin (Cheresh and Spiro, 1987), was analysed using B16 F1 melanoma cells expressing β3-integrin fused to green fluorescent protein [β3-GFP cells (Ballestrem et al., 2001)]. This integrin accumulated at vitronectin dots as did the focal adhesion molecules described above (Fig. 4E,F). Termination of actin bundles within these integrin clusters (Fig. 4F) as well as within clusters of focal adhesion-associated proteins (Fig. 4B) demonstrated firm anchorage of the cell.

The redistributions of focal adhesion-associated molecules and the actin cytoskeleton to the dot pattern strictly depended on proper signalling induced by ECM proteins. When seeded on micropatterned substrata with no ECM protein coating (no coating at all or BSA coating), cells neither adhered nor developed any typical adhesions sites. In contrast, when cells were plated on patterned polylysine substrata, they were able to adhere, but actin stress fibres connecting neighbouring dots were not formed. Instead, cells displayed an irregular morphology with numerous filopodia-like extensions (Fig. 5B) and clustering of focal adhesion molecules such as vinculin or paxillin was not observed (Fig. 5C). Together, these results suggest that typical focal adhesions form on ECM-coated substrata prepared with μCP. In addition, various cell types reacted to these patterned substrata by redistributing their integrin receptors, intracellular signal transduction molecules and cytoskeletal proteins during cellular spreading.

A distance of 25 μm between ECM dots is critical for cell spreading

We next determined the capacity of B16 cells to spread on ECM dots with increasing distance between them. Cells were plated on coverslips coated with patterned substrata of fibronectin and their actin cytoskeleton was visualised. On a homogeneous substratum prepared with μCP (Fig. 6A), cell spreading was comparable to that of cells plated on ECM-coated glass coverslips (not shown). As long as the spacing of dots was less than 2 μm (centre to centre), cell morphology was indistinguishable from that found on a homogeneous substratum (Fig. 6B,C) although bundles of actin filaments still terminated at the dots. With increasing distance between fibronectin dots (5-20 μm), cells adapted their shape to the dot pattern and displayed straight edges from dot to dot (Fig. 3, Fig. 6D-F). In these cells, the actin cytoskeleton formed stress fibres between adjacent dots (Fig. 3, Fig. 6D-F). Interestingly, actin fibres in the cellular periphery do usually not form

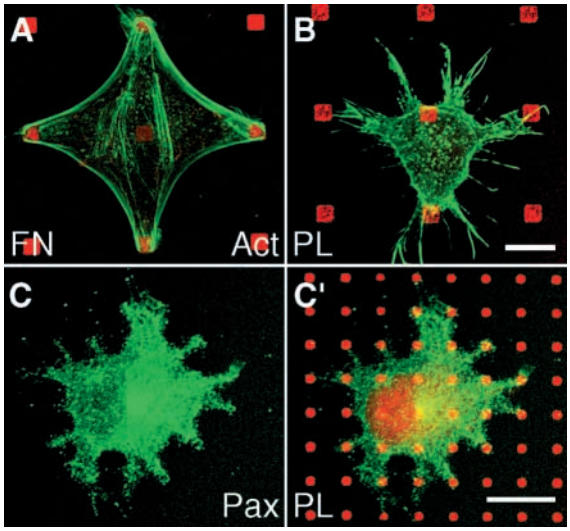

Fig. 5. Cell spreading on polylysine. B16 cells were cultured on patterned substrata of fibronectin (red; A) or polylysine (red; B,C) and labelled for actin (green; A,B) and paxillin (green; C). Cells can adhere to polylysine dots, however, the actin cytoskeleton is not reorganised (B) and paxillin does not accumulate over the dots (C). Scale bars: 10 μm.

straight lines between neighbouring dots but bend in a curved bundle towards the centre of the cell. When the distance between dots exceeded 25 μm, cell spreading was limited and the cells became triangular, ellipsoid or round (Fig. 6G-I). Quantification of all three investigated cell types revealed a critical spacing beyond which cells no longer spread (Table 1). With a spacing of ≤15 μm, more than 80% of plated cells spread over at least five dots. With a spacing of 20-25 μm, most cells spread over two to four dots. At 30 μm, cells adhered to one dot and did not spread.

This demonstrates that cells were able to bridge non-adhesive regions as large as 25 μm during cellular spreading. This distance could also be a limiting factor for cells spreading and migration in a complex tissue environment.

ECM-dots of 0.1 μm^2 induce intracellular signalling but do not support cell spreading when spaced at 5 μm

Focal adhesions that form on substrata uniformly coated with ECM proteins vary in size between 0.25 and 10 μm^2 and present either small, initial focal complexes (Nobes and Hall, 1995) or larger, mature focal contacts (Gumbiner, 1996; Balaban et al., 2001; Ballestrem et al., 2001). We investigated, whether the size of an ECM-coated area has an influence on the formation of focal adhesions and on cell spreading. Cells were plated for 1 hour on patterned substrata with dot sizes from 0.1 to 1 μm^2 and a constant spacing of 5 μm (centre to centre). All three investigated cell types readily spread on dots that were 0.25 μm^2 or larger. In these cells, the actin cytoskeleton formed normal stress fibres connecting the dots (Fig. 7A). A dot surface of 0.1 μm^2 still allowed cell adhesion but the cells no longer spread (Fig. 7A).

In principle, dots of 0.1 μm^2 could be too small to be recognised by a cell as an adhesive dot. However, cells spreading on 0.1 μm^2 dots accumulated markers for

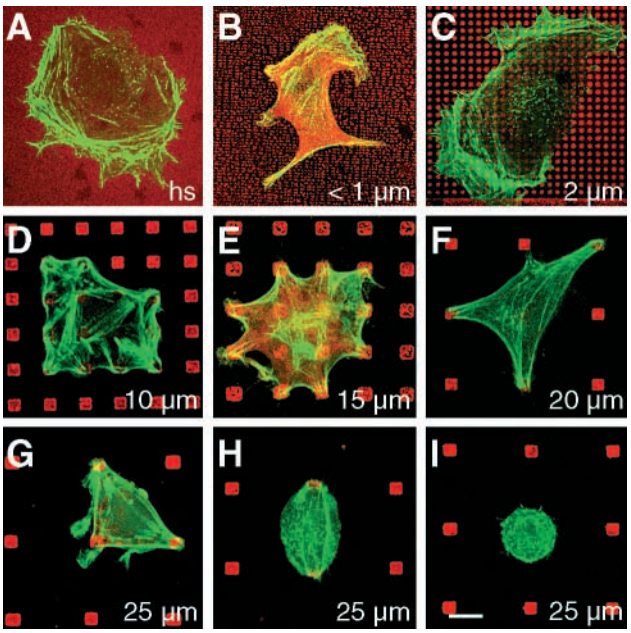

Fig. 6. Cell spreading in relation to substratum geometry. B16 cells were cultured on fibronectin substrata prepared with μCP and labelled for fibronectin (red) and actin (green). (A) On a homogeneous substratum (hs), actin filaments are distributed throughout the cell periphery. (B,C) If the space between dots is ≤2 μm (B: 0.1 μm^2 squares 1 μm apart, C: 1 μm^2 squares 2 μm apart) cells spread as on a homogeneous substratum. (D-I) Cell growth on patterned substrata of 9 μm^2 dots with spacing as indicated in the right-hand corner. (D-F) With distances of 5-20 μm between dots, cells spread and the actin cytoskeleton formed stress fibres between adjacent dots. (G-I) At a distance of 25 μm, spreading was limited and cells became triangular, ellipsoid or round. Scale bar: 10 μm.

intracellular signalling (phosphotyrosine, Fig. 7B) and focal adhesion molecules like vinculin (not shown) and paxillin (Fig. 7C). This indicates that the size of cell contact sites is determined by the microenvironment and can be much smaller than previously described in the literature.

The failure of cells to spread on 0.1 μm^2 dots with 5 μm spacing is therefore not because this ECM-coated area is too small to induce intracellular signalling. Cells can spread on

Table 1. Cell adhesion and spreading on different substrata geometries

	Spacing between dots (μm)							
Dot size (μm^2)	1	2	5	10	15	20	25	30
0.1	A, S	A, S	a, ns	na, ns				
0.25		A, S	a, s	a, ns				
1			A, S	a, s	a, s	a, s		
9				A, S	A, S	a, s	a, s	a, ns

Cells were cultured for 1 hour on patterned substrata and labelled for actin. The number of adhering cells (B16, 3T3 and BRL) and their spreading areas (B16, 3T3) were analysed.

A, number of adhering cells similar to that on homogenous substrata; a, number of adhering cells smaller than on homogenous substrata; na, no adhesion; S, spreading area 50% or larger than on homogenous substrata; s, spreading area less than 50% of that on homogenous substrata; ns, spreading area as on uncoated substrata.

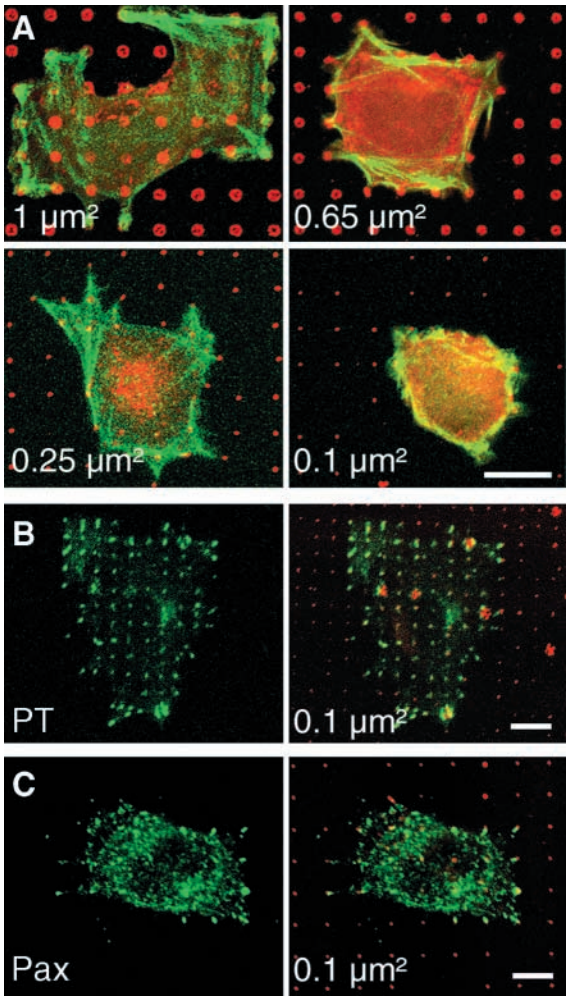

Fig. 7. Fibronectin dots of 0.1 μm² induce intracellular signalling but do not support cell spreading at distances >5 μm. (A) B16 cells growing on patterned fibronectin substrata with varying dot sizes (as indicated in the lower left corner) and a constant spacing of 5 μm (centre to centre). Cells spread and form actin stress fibres on dots down to 0.25 μm². On 0.1 μm² dots, cells adhere but do not spread. Note missing dots in the vicinity of the cells on 0.25 μm² and 0.1 μm² substrata. Scale bar: 10 μm. (B) A cell sitting on 0.1 μm² dots at a spacing of 2 μm. Phosphotyrosine (PT, green) accumulates in areas of the cell overlying fibronectin dots (red) indicating that an area of 0.1 μm² is sufficient to induce intracellular signalling. (C) Staining for paxilin (Pax, green) of a cell sitting on 0.1 μm² fibronectin dots (red) separated by distances of 4 μm. Like phosphotyrosine, paxilin accumulates over small dots. Scale bars: 5 μm.

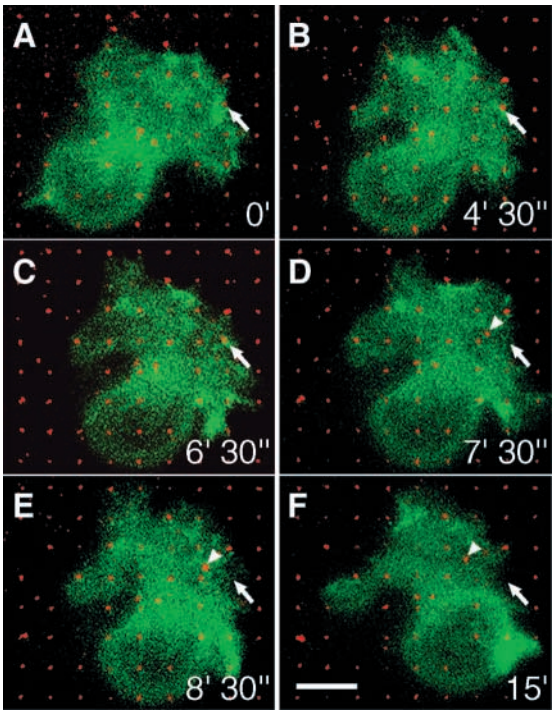

Fig. 8. Dynamics of cell spreading on fibronectin dots of 0.1 μm². Images of a time-lapse sequence of a B16 cell expressing β3-integrin-GFP (β3-GFP) growing on a patterned substratum of 0.1 μm² fibronectin dots. Dots were visualised by mixing the fibronectin with fluorescently labelled BSA. Since β3-GFP cells display homogeneous background fluorescence, they were used in these assays to reveal cell morphology. The cell was highly motile but did not spread. A few minutes after initial contact, a dot (arrows in A-F) was first stretched (arrow in C), removed from the substratum (arrowhead in D) and then internalised into the cell (arrowheads in E and F). This behaviour results in a rearranged dot pattern after a cell has migrated over that area. Time is given in minutes and seconds. Scale bar: 10 μm.

0.1 μm² dots with 1 or 2 μm spacing (Fig. 6B, Fig. 7B), but we noted that on substrata with small dots and 5 μm spacing, single dots were either displaced or missing (Fig. 7A). Missing dots were rarely observed in the vicinity of cells on substrata with 0.25 μm² dots, however, this phenomenon was typical for substrata with 0.1 μm² dots. To analyse this phenomenon in more detail, cells were plated onto patterned substrata and imaged with time-lapse videomicroscopy. Since β3-GFP cells displayed homogeneous membrane fluorescence, they were used in these assays to reveal cell morphology. We observed, that cells on substrata with dots of 0.25 μm² or larger adhered and extended lamellipodia. These lamellipodia became stabilised after contact with ECM dots and the cells easily spread (not shown). In contrast, cells on patterned substrata with 0.1 μm² dots (5 μm spacing) were highly motile but did not spread. A few minutes after initial contact, 0.1 μm² dots were first laterally displaced, removed from the substratum and then internalised into the cell (Fig. 8C). This behaviour results in a rearranged dot pattern after a cell has migrated over that area (Fig. 8F). This suggests that the force applied by a single focal adhesion is stronger than the hydrophobic interactions binding fibronectin to the surface. That would also suggest that the limits of cell spreading in our system are due to mechanical and not to signalling limits.

Our findings indicate that cells can properly adhere to and spread on patterned ECM-coated areas equal to or larger than 0.25 μm² spaced at 5 μm. Smaller dots of 0.1 μm² spaced at 5 μm support adhesion but not spreading of cells. However, cells were able to spread on dots of 0.1 μm² if the spacing was reduced. A summary of cell behaviour in relation to the investigated substratum patterns is given in Table1.

A fibronectin surface coverage of 15% is essential for cell spreading

An alternative explanation for the absence of cell spreading on 0.1 μm^2 dots spaced at 5 μm (0.4% substratum coverage) could be the insufficient stimulation of the spreading lamellipodia by the widely spaced small sized focal adhesions. If the spacing between these small contacts was reduced to 1 μm (9% substratum coverage), spreading was probably caused by the production of second messengers beyond the threshold required for spreading. We therefore tested whether there was a correlation between cell surface coverage of ECM molecules and the extent of cellular spreading. The area covered by NIH/3T3 and B16 cells (10 cells/pattern) was measured on different patterns with a variable fibronectin surface coverage, on uncoated substrata (0% FN coverage) and on homogeneous fibronectin substrata (100% FN coverage). Fig. 9A,B illustrates that cells adhering to an uncoated substratum covered an area of 202±17 μm^2 (NIH/3T3) and 232±22 μm^2 (B16), respectively, whereas cells on a homogeneous substratum spread over an area of 1623±75 μm^2 (NIH/3T3) and 1447±127 μm^2 (B16), respectively. Half maximal spreading was reached at a 5-8% coverage of the surface with fibronectin for both cell types. At a surface coating above 15%, optimal spreading (80% maximal spreading) was attained.

These findings indicate that cell spreading is directly correlated to the substratum coverage with ECM proteins, but irrespective of the geometrical pattern. The spreading/coverage relationship is further sustained by comparing three differently patterned substrata that all have an effective fibronectin coverage of 4% but different geometries (Fig. 9B,C, arrow). Cells spreading on a pattern with dots 4 μm square at a distance of 16 μm (margin to margin) covered an area of 609±60 μm^2. This area is statistically not distinguishable (U-test after Mann-Whitney) from values measured on substrata with dots of 2 μm square at a distance of 8 μm (564±46 μm^2) and on substrata with dots of 1 μm square at a distance of 4 μm (611±40 μm^2).

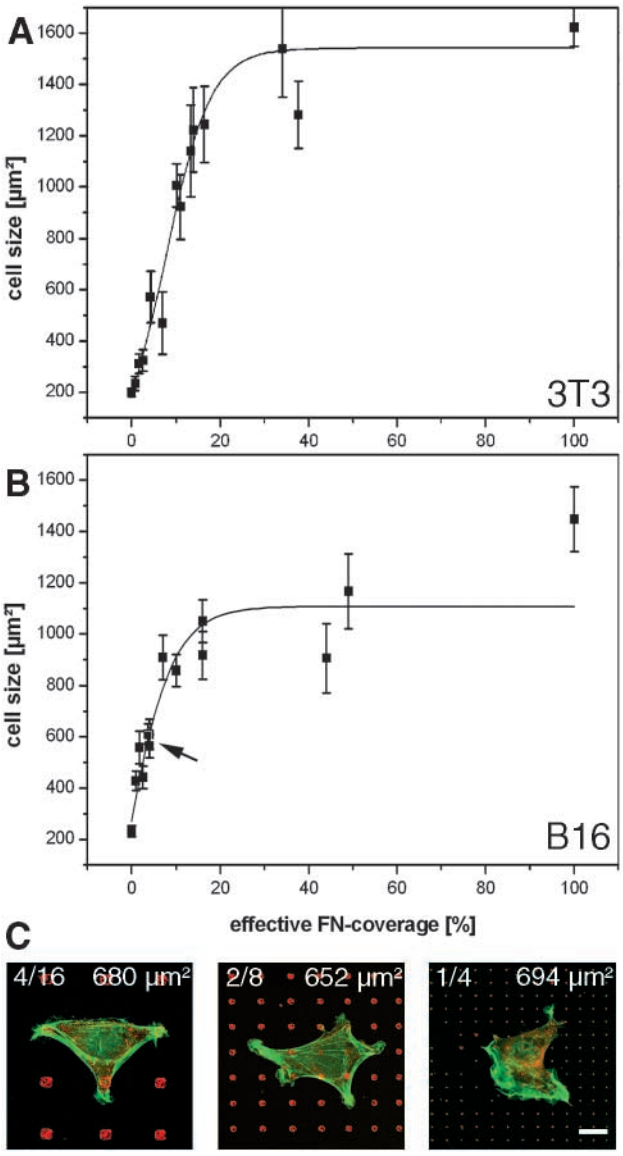

Fig. 9. Correlation between cell spreading and substratum coating. (A,B) The area covered by NIH/3T3 cells (A) and B16 cells (B) that have spread was plotted against the actual fibronectin surface for 12 different dot patterns, uncoated and homogeneously coated substrata. Bars represent s.e.m. (C) Three representative cells from patterns with 4% fibronectin coverage (arrow in B). Cell sizes as indicated in the upper right-hand corner were almost equal despite the different fibronectin patterns (actual length and margin to margin distance of dots is given in μm in the upper left corner).

Selected dot usage by cells

Whereas cells could adhere equally well to dots 1-3 μm square when spaced below 25 μm, the amount of dot-area covered with focal adhesion proteins varied in relation to the actual dot area. FAK (Fig. 4C), phosphotyrosine (Fig. 4D), paxillin (Fig. 4E′) and β3-integrin (Fig. 4E) were found clustered directly over the entire surface of dots 1 μm square. Vinculin was often laterally associated with the focal adhesions formed over the dots and was extending along actin stress fibres towards the interior of the cells (Fig. 4B). The vinculin stretches were usually connected to one or two thicker actin bundles (Fig. 4B) pointing in the same direction. Beginning with dots 2 μm square and clearly visible with dots 3 μm square, the distribution of focal adhesion-associated molecules changed. All investigated molecules now clustered around the edges of the dots (Fig. 10). On dots at the cellular periphery, the dot margins facing the periphery were usually more strongly labelled than the margins oriented towards the centre of the cell (Fig. 10). Actin bundles were often connected to the outer margins of the dots and pointed in two to three different directions (Fig. 10).

To quantify dot usage by cells in relation to dot size, we choose two representative antigens: phosphotyrosine as a marker for intracellular signalling and paxillin as a focal adhesion-associated molecule. B16 cells were cultured for 1 hour on patterned substrata and immunolabelled for fibronectin, actin and phosphotyrosine (or paxillin). Under these conditions B16 cells form small, dot-like or elongated contacts in peripheral regions of the lamellipodia when growing on homogenous substrata prepared with μCP. The average size of these contacts measured 0.66±0.15 μm^2 (min: 0.34; max: 1.05) for phosphotyrosine (Fig. 10A) and 0.28±0.04 μm^2 (min: 0.13; max: 0.6) for paxillin (Fig. 10B).

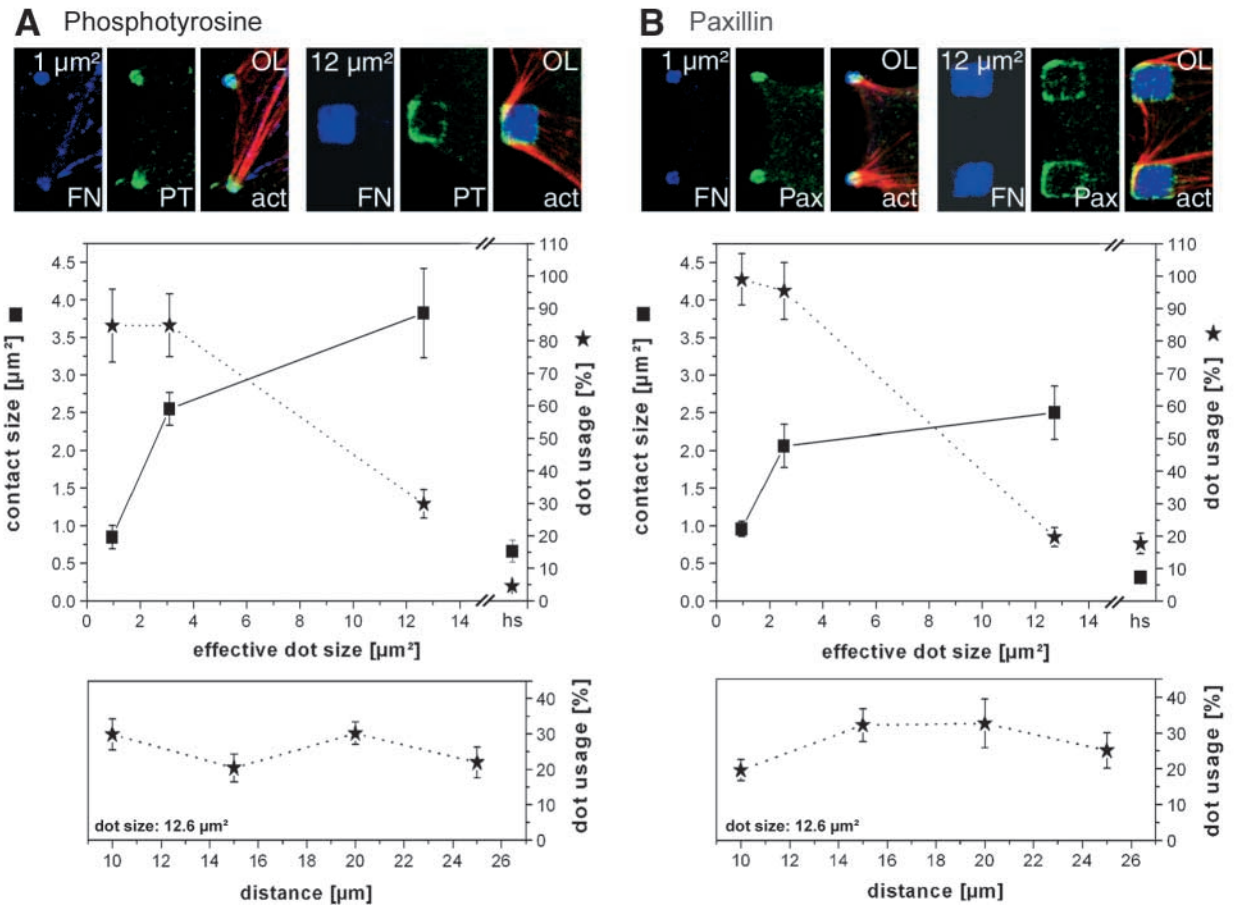

Fig. 10. Quantification of dot usage. B16 cells were cultured for 1 hour on patterned substrata and labelled for fibronectin (FN), actin (act) and phosphotyrosine (PT) or paxillin (Pax). The area covered by phosphotyrosine (A) or paxillin (B) was measured for focal adhesions in the cellular periphery for cells growing on homogeneous substrata (hs) and on patterned substrata with three different dot sizes (contact size, ■) and set in relation to the underlying fibronectin area (dot usage, ★). Dot usage was also determined for focal adhesions formed on patterned substrata with 12 µm^2 dots and variable distances. Bars represent s.e.m.

The areas covered by phosphotyrosine or paxillin were measured for contacts on patterned substrata with dot sizes of 1, 3, and 12 µm^2 spaced at 10 µm. Since cells were cultured on gold-coated coverslips, they could only be imaged with epifluorescence from the upper surface. To exclude the possibility that fluorescence intensity might be quenched by thicker parts of the cells, only peripheral contacts were analysed. As shown in Fig. 10, the size of the focal adhesions increased with actual dot size measured by phosphotyrosine and paxillin localisation. However, the relative dot coverage [expressed as contact size × 100 / underlying fibronectin area (%)] dropped from 90% on 1 and 3 µm^2 dots to 20-30% on 12 µm^2 dots. A similar low degree of substratum usage (below 20%) was also found underneath peripheral lamella in cells growing on homogeneous fibronectin substrata (Fig. 10).

We next determined, whether use of 12 µm^2 dots changed with dot distance and thus depended on the plasma membrane surface and cytoplasmic volume from which focal adhesion molecules have to be recruited in order to form focal adhesions on the dot. However, the percentage of dot area covered either by phosphotyrosine or paxillin remains constant, independent of whether dots are 10, 15, 20 or 25 µm apart (Fig. 10) (corresponding to an ECM coverage of 9, 4, 2.25 and 1.44%). These findings suggest that the maximal size of a focal adhesion in B16 cells is determined by cell intrinsic factors such as the amount of intracellular tension (Balaban et al., 2001) and is not limited by the amount of available focal adhesion molecules and/or ECM surface.

Discussion

The main objective of the present study was to elucidate the influence of ECM distribution on the initial process of cell spreading and attachment. Using µCP, we created different geometrical patterns of fibronectin and vitronectin in the submicrometer range. We demonstrate that cells cultured on these substrata integrate the lattice to which they are exposed in order to maintain their shape and to regulate adhesion and spreading. The adaptation occurs within a limited range of surface coverage and ECM spacing.

The interaction of cells with microengineered substrata has been extensively studied over the past decades (reviewed by Folch and Toner, 2000). Microfabrication technologies and geometries of the substrata used ranged from three-dimensional patterns in grooved quartz surfaces (den Braber et al., 1998) to surfaces micropatterned with bioactive peptides

(Matsuzawa et al., 1996). However, most of these studies used patterns ranging between 5-100 μm and cell behaviour as a whole was analysed rather than subcellular reactions. Ingber and co-workers (Chen et al., 1997; Chen et al., 1998) were the first to investigate whether the critical parameter in the switching of endothelial cells between growth and apoptosis is the total area of ECM contact or the projected cell spread area. Using μCP, they produced arrays of 3 or 5 μm fibronectin dots interspersed with non-adhesive regions and thus were able to control cell spreading independently of the total cell surface area. With this experimental set-up they could show that cell shape and not ECM contact area determines cellular fate.

The technological details and biological applications of μCP have been extensively discussed elsewhere (LeDuc et al., 2002; Mrksich and Whitesides, 1996). In summary, μCP is a versatile method for producing geometrically defined patterns of a variety of proteins. Since the proteins adsorb to the surface from physiological buffer solutions, their biological activity is generally preserved. A major disadvantage of the technique is the poorly defined surface chemistry. Proteins adsorb via hydrophobic interactions to the surface in random orientations that cannot be controlled experimentally. In addition, the binding strengths of proteins to the hydrophobic surface are currently unknown. We have studied protein adsorption in more detail with AFM and found that 50% of the dot surface is covered with a monolayer of tightly adhering fibronectin. As thickness (3 nm) and length (130 nm) of isolated fibronectin molecules have been determined (Engel et al., 1981), we can estimate a surface coverage of 1000 molecules/μm^2 in our experiments. However, since these molecules are bound in a random orientation to the surface, the number of available binding sites for integrin receptors might be much lower.

We observed that with increasing dot size, focal adhesions began to form at the edge of the dots, where the ECM- covered surface meets the non-adhesive surface. This finding is consistent with the recent demonstration that traction forces are concentrated within the corners of smooth muscle cells cultured on 50 μm square adhesive islands (Wang et al., 2002). A similar pattern for vinculin was also described in endothelial cells growing on 5 μm square fibronectin islands (Chen et al., 1997; Brock et al., 2003). The distribution of cell matrix adhesion molecules and the trajectories of the associated actin fibres might therefore reflect the balance between cellular traction forces and the availability of potential adhesion sites. We propose, that this 'edge effect' is caused by the non-linear resistance created by the adhesive dot surface within the inward directed, acto-myosin-dependent intracellular force field. It has been recently demonstrated that local induction of mechanical tension leads to reinforcement of focal adhesions (Lo et al., 2000; Riveline et al., 2001; Geiger and Bershadsky, 2002; Wehrle-Haller and Imhof, 2002). The focal adhesion components (integrin and adapter proteins) localised directly at the edge of the dot take the biggest mechanical load. It has been demonstrated that the increase in mechanical load on pre-existing focal adhesions results in the formation of binding sites that allow the further recruitment of structural and signalling focal adhesion components (Sawada and Sheetz, 2002).

We have shown that cells react to fibronectin dots as small as 0.1 μm^2 by enhanced intracellular signalling, the accumulation of focal adhesion molecules and the application of traction forces. These findings indicate firm anchorage of the actin cytoskeleton. A prerequisite for attachment of the cytoskeleton to focal adhesions is the clustering of integrin receptors (Miyamoto et al., 1995). Using beads coated with fragments of fibronectin, it has been shown that clusters of three integrin-binding ligands are sufficient to mechanically couple the integrins to the actin cytoskeleton (Coussen et al., 2002). With a fibronectin coverage of about 1000 molecules/μm^2, there should be enough integrin-binding sites available on dots of 0.1 μm^2 to induce an integrin coupling to the actin cytoskeleton. That cells were unable to spread on 0.1 μm^2 dots spaced 5 μm apart therefore seems to be a shortcoming of the μCP technique. Since cells remove and internalise the complete fibronectin dots after initial contact, the most plausible explanation is that the hydrophobic interactions binding fibronectin to the alkenethiols are weaker than the cellular traction forces applied to small isolated contacts. These adhesions therefore behave like nascent focal adhesions formed in migrating fibroblasts, which can generate strong propulsion forces independent of their small size (Beningo et al., 2001). However, since binding forces of fibronectin to the hydrophobic surface are not known, we were unable to estimate the forces involved in dot removal.

An alternative explanation for the inability for cells to spread on 0.1 μm^2 dots spaced 5 μm apart could be related to the signalling cascade that initiates the spreading process. In the absence of serum, cells rely uniquely on the clustering of their cell surface-expressed integrins to initiate a Rac1-dependent spreading process. This pathway involves the activation of FAK by integrin clustering and the local production of phosphoinositides (Price et al., 1997). In the case of a very dilute presentation of ECM protein covered dots, the spreading signal emitted by a 0.1 μm^2 focal adhesion may be too weak to induce lamellipodial extension leading to precocious retraction of extending cellular processes.

Based on these ideas we might consider three different stages of cell spreading that each require a distinct amount of available ECM molecules. The first step involves cell-substratum adhesion that can be mediated in an integrin-independent manner, as exemplified by the attachment of cells on polylysine-coated substrata. A second step involves the clustering of integrins and the formation of focal complexes in the spreading lamellipodia. This step is associated with the assembly of focal adhesion structures and the FAK-dependent spreading of cells (Ren et al., 2000) that involves the activation of Rac1 and Cdc42, leading to the formation of lamellipodia and filopodia required for spreading. After the Rac1-dependent spreading step, the third step of cell adhesion is initiated by the activation of RhoA and the formation of actin stress fibres and the development of intracellular tension (Nobes and Hall, 1995).

Based on our results, an ECM coverage equal to 0.4% and a dot sizes of 0.1 μm^2 stimulates lamellipodia formation and extension, however, the subsequent Rho-dependent retraction process and focal contact maturation requires an ECM coverage of 5-8%. In the presence of ECM dots that exceed 3 μm^2, cells use only a fraction of the dot surface for the formation of focal adhesions. This suggests that during the Rho-dependent attachment process cells need only a fraction of the 5-8% surface coverage for effective adhesion, but require ECM substrata at high local concentrations.

While analysing cellular behaviour on the patterned substrata we noted the existence of three different thresholds that affected cellular behaviour. The first threshold is determined by the fibronectin dot density. During cell spreading and subsequent formation of focal contacts and stress fibres on a homogeneously coated substratum, cells seem to form adhesions in a seemingly random pattern. However, when distance increases between ECM substratum sites, cell spreading and subsequent adhesion is dictated by the available pattern. We observed that dot distances of ≥5 μm had an impact on cellular shape, while at distances of ≤2 μm cells behaved as on a homogeneous substratum. Since cellular shape is determined by the intracellular tension generated by the actin cytoskeleton anchored between focal adhesion sites, the rigidity (i.e. stiffness) of the actin cables between ECM binding sites at distances of ≤2 μm might be higher than the respective force generated at this distance. Alternatively, closely spaced focal adhesions are functionally interconnected in order to integrate and withstand high cellular forces required for migration. In contrast, isolated focal adhesions found for example at the rear of migrating cells are exposed to a much higher local force. Owing to force integration between closely spaced focal adhesions (≤2 μm) a higher density of focal adhesions in the front of migrating cells can induce pulling forces that outnumber individual focal adhesions at the cell rear (Beningo et al., 2001). In turn this integration threshold will make it extremely difficult to measure pulling forces on closely spaced individual focal adhesions with commonly used systems based on elastic substrata (Harris et al., 1980; Balaban et al., 2001; Beningo and Wang, 2002).

A second threshold for cell spreading is determined by the maximal fibronectin dot-distance. At a dot distance above 25 μm, the analysed cell types were no longer able to bridge the nonadhesive substratum with either lamellipodia or filopodia, in order to spread completely. At this distance the polymerising and self-organising activity of the actin cytoskeleton is no longer able to support and stabilise these sensory organelles of a spreading or migrating cell. While 30 μm seems to be the limit for mesenchymal type of cells, neuronal cells, which are able to form specialised protrusive organelles such as growth cones, may be able to bridge even wider non-adhesive surfaces (Hammarback and Letourneau, 1986).

A third threshold is determined by the surface coverage with fibronectin. In our experiments surface coverage is defined by a combination of dot size and dot distance. We found that the extent of cell spreading is directly correlated to the total substratum coverage with ECM proteins, but independent of the geometrical pattern. This indicates that cells integrate the amount of ECM proteins to which they are exposed and react by adjusting their rate of spreading. An alternative way to seek the threshold for cell adhesion would consist of diluting monovalent integrin ligands until cells will no longer adhere (Massia and Hubbell, 1991; Koo et al., 2002; Wehrle-Haller and Imhof, 2002). This technique however, identifies the substratum density limits required to form focal adhesion per se. Microcontact printing allows the analysis of completely functional adhesion sites and their influence on cell behaviour. In vivo, ECM substrata are likely to be distributed in complex non-linear patterns. Large non-adhesive regions alternate with high-density aggregates with a high integrin binding density. For the design of artificial cell-interacting surfaces, the control of integrin ligand density at the nanometer range, as well as the spacing of ECM ligand patches at the micrometer range will be required to control cell adhesion as well as cell shape.

In summary, patterning substrata with ECM molecules in the submicrometer range proved to be a valuable tool for studying the early events of cell adhesion and cell spreading. Combining these methods with other approaches, such as green-fluorescent protein imaging and gene manipulation, will be particularly powerful for analysing the dynamics of focal adhesion assembly.

EG3Me was kindly provided by Dr Eck, University of Heidelberg. We thank Mary A. Cahill for helpful comments on an earlier version, Rainer Fuchs for initial experiments and Ulrike Binkle for technical assistance. The work was supported by the Deutsche Forschungsgemeinschaft (SFB 513) and the Fond der Chemischen Industrie (to M.B.). M.B. was a Heisenberg Fellow of the DFG. This article is dedicated to my father, the late Dr Walter Bastmeyer.

References

Abrams, G. A., Goodman, S. L., Nealey, P. F., Franco, M. and Murphy, C. J. (2000). Nanoscale topography of the basement membrane underlying the corneal epithelium of the rhesus macaque. *Cell Tissue Res.* **299**, 39-46.

Balaban, N. Q., Schwarz, U. S., Riveline, D., Goichberg, P., Tzur, G., Sabanay, I., Mahalu, D., Safran, S., Bershadsky, A., Addadi, L. and Geiger, B. (2001). Force and focal adhesion assembly: a close relationship studied using elastic micropatterned substrata. *Nat. Cell Biol.* **3**, 466-472.

Ballestrem, C., Wehrle-Haller, B. and Imhof, B. A. (1998). Actin dynamics in living mammalian cells. *J. Cell Sci.* **111**, 1649-1658.

Ballestrem, C., Hinz, B., Imhof, B. A. and Wehrle-Haller, B. (2001). Marching at the front and dragging behind: differential alphaVbeta3- integrin turnover regulates focal adhesion behaviour. *J. Cell Biol.* **155**, 1319-1332.

Beningo, K. A., Dembo, M., Kaverina, I., Small, J. V. and Wang, Y. L. (2001). Nascent focal adhesions are responsible for the generation of strong propulsive forces in migrating fibroblasts. *J. Cell Biol.* **153**, 881-888.

Beningo, K. A. and Wang, Y. L. (2002). Flexible substrata for the detection of cellular traction forces. *Trends Cell Biol.* **12**, 79-84.

Brock, A., Chang, E., Ho, C. C., LeDuc, P., Jiang, X., Whitesides, G. M. and Ingber, D. E. (2003). Geometric determinants of directional cell motility revealed using microcontact printing. *Langmuir* **19**, 1611-1617.

Burridge, K. and Chrzanowska-Wodnicka, M. (1996). Focal adhesions, contractility, and signaling. *Annu. Rev. Cell Dev. Biol.* **12**, 463-518.

Chen, C. S., Mrksich, M., Huang, S., Whitesides, G. M. and Ingber, D. E. (1997). Geometric control of cell life and death. *Science* **276**, 1425-1428.

Chen, C. S., Mrksich, M., Huang, S., Whitesides, G. M. and Ingber, D. E. (1998). Micropatterned surfaces for control of cell shape, position, and function. *Biotechnol. Prog.* **14**, 356-363.

Cheresh, D. A. and Spiro, R. C. (1987). Biosynthetic and functional properties of an Arg-Gly-Asp-directed receptor involved in human melanoma cell attachment to vitronectin, fibrinogen, and von Willebrand factor. *J. Biol. Chem.* **262**, 17703-17711.

Coussen, F., Choquet, D., Sheetz, M. P. and Erickson, H. P. (2002). Trimers of the fibronectin cell adhesion domain localize to actin filament bundles and undergo rearward translocation. *J. Cell Sci.* **115**, 2581-2590.

Cukierman, E., Pankov, R., Stevens, D. R. and Yamada, K. M. (2001). Taking cell-matrix adhesions to the third dimension. *Science* **294**, 1708-1712.

David, C. and Hambach, D. (1999). Line width control using a defocused low voltage electron beam. *Microelectronic Engineering* **46**, 219-222.

David, C. and Souvorov, A. (1999). High efficiency Bragg-Fresnel lenses with 100 nm outermost zones width. *Rev. of Sci. Instrum.* **70**, 4168-4173.

den Braber, E. T., de Ruijter, J. E., Ginsel, L. A., von Recum, A. F. and Jansen, J. A. (1998). Orientation of ECM protein deposition, fibroblast cytoskeleton, and attachment complex components on silicone microgrooved surfaces. *J. Biomed. Mater. Res.* **40**, 291-300.

Engel, J., Odermatt, E., Engel, A., Madri, J. A., Furthmayr, H., Rohde, H. and Timpl, R. (1981). Shapes, domain organizations and flexibility of laminin and fibronectin, two multifunctional proteins of the extracellular matrix. *J. Mol. Biol.* **150**, 97-120.

Folch, A. and Toner, M. (2000). Microengineering of cellular interactions. *Annu. Rev. Biomed. Eng.* **2**, 227-256.

Geiger, B., Bershadsky, A., Pankov, R. and Yamada, K. M. (2001). Transmembrane crosstalk between the extracellular matrix–cytoskeleton crosstalk. *Nat. Rev. Mol. Cell. Biol.* **2**, 793-805.

Geiger, B. and Bershadsky, A. (2002). Exploring the neighborhood: adhesion-coupled cell mechanosensors. *Cell* **110**, 139-142.

Geissler, M., Bernard, A., Bietsch, A., Schmidt, H., Michel, B. and Delamarche, E. (2000). Microcontact-printing chemical patterns with flat stamps. *J. Am. Chem. Soc.* **122**, 6303-6304.

Gumbiner, B. M. (1996). Cell adhesion: the molecular basis of tissue architecture and morphogenesis. *Cell* **84**, 345-357.

Hammarback, J. A. and Letourneau, P. C. (1986). Neurite extension across regions of low cell-substratum adhesivity: implications for the guidepost hypothesis of axonal pathfinding. *Dev. Biol.* **117**, 655-662.

Harris, A. K., Wild, P. and Stopak, D. (1980). Silicone rubber substrata: a new wrinkle in the study of cell locomotion. *Science* **208**, 177-179.

Hynes, R. O. (1992). Integrins: versatility, modulation, and signaling in cell adhesion. *Cell* **69**, 11-25.

Ingber, D. E. (1997). Tensegrity: the architectural basis of cellular mechanotransduction. *Annu. Rev. Physiol* **59**, 575-599.

James, C. D., Davis, R. C., Kam, L., Craighead, H. G., Isaacson, M., Turner, J. N. and Shain, W. (1998). Patterned proteins layers on solid substrata by thin stamp microcontact printing. *Langmuir* **14**, 741-744.

Koo, L. Y., Irvine, D. J., Mayes, A. M., Lauffenburger, D. A. and Griffith, L. G. (2002). Co-regulation of cell adhesion by nanoscale RGD organization and mechanical stimulus. *J. Cell Sci.* **115**, 1423-1433.

LeDuc, P., Ostuni, E., Whitesides, G. M. and Ingber, D. E. (2002). Use of micropatterned adhesive surfaces for control of cell behaviour. *Methods Cell Biol.* **96**, 385-401.

Lo, C. M., Wang, H. B., Dembo, M. and Wang, Y. L. (2000). Cell movement is guided by the rigidity of the substratum. *Biophys. J.* **79**, 144-152.

Massia, S. P. and Hubbell, J. A. (1991). An RGD spacing of 440 nm is sufficient for integrin alpha V beta 3-mediated fibroblast spreading and 140 nm for focal contact and stress fiber formation. *J. Cell Biol.* **114**, 1089-1100.

Matsuzawa, M., Liesi, P. and Knoll, W. (1996). Chemically modifying glass surfaces to study substratum-guided neurite outgrowth in culture. *J. Neurosci. Methods* **69**, 189-196.

Miyamoto, S., Teramoto, H., Coso, O. A., Gutkind, J. S., Burbelo, P. D., Akiyama, S. K. and Yamada, K. M. (1995). Integrin function: molecular hierarchies of cytoskeletal and signaling molecules. *J. Cell Biol.* **131**, 791-805.

Mrksich, M. and Whitesides, G. M. (1996). Using self-assembled monolayers to understand the interactions of man-made surfaces with proteins and cells. *Annu. Rev. Biophys. Biomol. Struct.* **25**, 55-78.

Mrksich, M., Dike, L. E., Tien, J., Ingber, D. E. and Whitesides, G. M. (1997). Using microcontact printing to pattern the attachment of mammalian cells to self-assembled monolayers of alkanethiolates on transparent films of gold and silver. *Exp. Cell Res.* **235**, 305-313.

Nobes, C. D. and Hall, A. (1995). Rho, rac, and cdc42 GTPases regulate the assembly of multimolecular focal complexes associated with actin stress fibers, lamellipodia, and filopodia. *Cell* **81**, 53-62.

Price, L. S., Leng, J., Schwartz, M. A. and Bokoch, G. M. (1997). Activation of Rac and Cdc42 by integrins mediates cell spreading. *Mol. Biol. Cell* **9**, 1863-1871.

Prime, K. L. and Whitesides, G. M. (1991). Self-assembled organic monolayers: model systems for studying adsorption of proteins at surfaces. *Science* **252**, 1164-1167.

Ren, X. D., Kiosses, W. B., Sieg, D. J., Otey, C. A., Schlaepfer, D. D. and Schwartz, M. A. (2000). Focal adhesion kinase suppresses Rho activity to promote focal adhesion turnover. *J. Cell Sci.* **113 (Pt 20)**, 3673-3678.

Riveline, D., Zamir, E., Balaban, N. Q., Schwarz, U. S., Ishizaki, T., Narumiya, S., Kam, Z., Geiger, B. and Bershadsky, A. D. (2001). Focal Contacts as Mechanosensors. Externally applied local mechanical force induces growth of focal contacts by an mdia1-dependent and rock-independent mechanism. *J. Cell Biol.* **153**, 1175-1186.

Sawada, Y. and Sheetz, M. P. (2002). Force transduction by Triton cytoskeletons. *J. Cell Biol.* **156**, 609-615.

Sheetz, M. P., Felsenfeld, D. P. and Galbraith, C. G. (1998). Cell migration: regulation of force on extracellular-matrix-integrin complexes. *Trends Cell Biol.* **8**, 51-54.

Wang, N., Ostuni, E., Whitesides, G. M. and Ingber, D. E. (2002). Micropatterning tractional forces in living cells. *Cell Motil. Cytoskeleton* **52**, 97-106.

Wehrle-Haller, B. and Imhof, B. A. (2002). The inner lives of focal adhesions. *Trends Cell Biol.* **12**, 382-389.

Wezeman, F. H. (1998). Morphological foundations of precartilage development in mesenchyme. *Microsc. Res. Tech.* **43**, 91-101.

Yamada, K. M. and Miyamoto, S. (1995). Integrin transmembrane signaling and cytoskeletal control. *Curr. Opin. Cell Biol.* **7**, 681-689.

Zamir, E. and Geiger, B. (2001). Molecular complexity and dynamics of cell-matrix adhesions. *J. Cell Sci.* **114**, 3583-3590.